Supplementary Information

Melamine-formaldehyde Resin Nanospheres Interlayer as "Li^+ Redistributor" to Stabilize Li Metal Anodes

Liang He,[ab] Qingjuan Ren,*[ab] Peng Zhang,[ab] Yujia Wang,[ab] Ruirui Hao,[ab] Kai Liu, and Zhiqiang Shi*[ab]

[a.] *Tianjin Key Laboratory of Advanced Fibers and Energy Storage, School of Materials Science and Engineering, Tiangong University, Tianjin 300387, China. E-mail: renqingjuan@tiangong.edu.cn; shizhiqiang@tiangong.edu.cn*

[b.] *Cangzhou Institute of Tiangong University, Cangzhou 061000, China.*

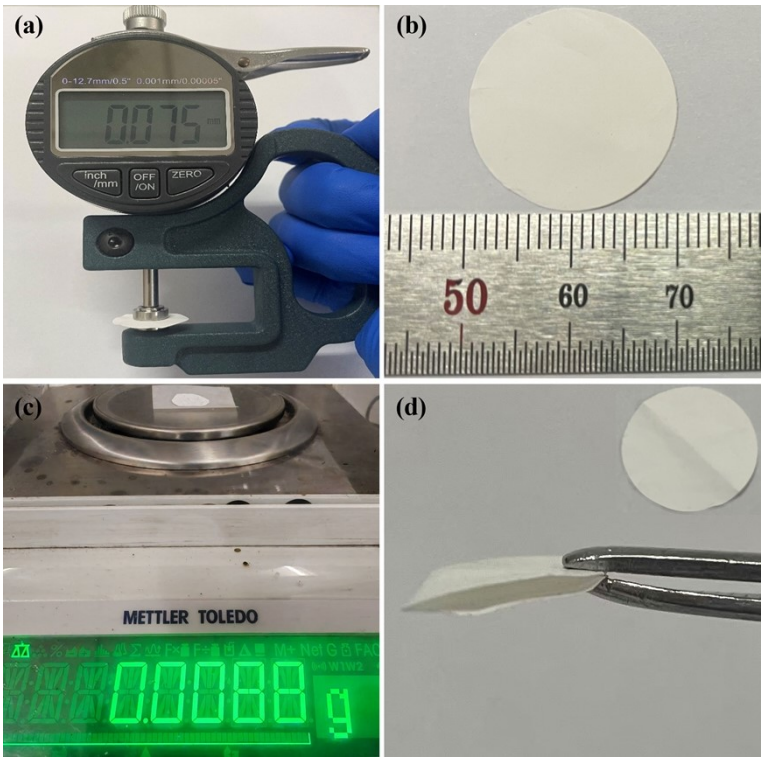

Fig. S1 Digital photos of MFNS. (a) Thickness, (b) diameter size, (c) weight, and (d) flexibility.

Fig. S2 Contact angle tests for MFNS interlayer.

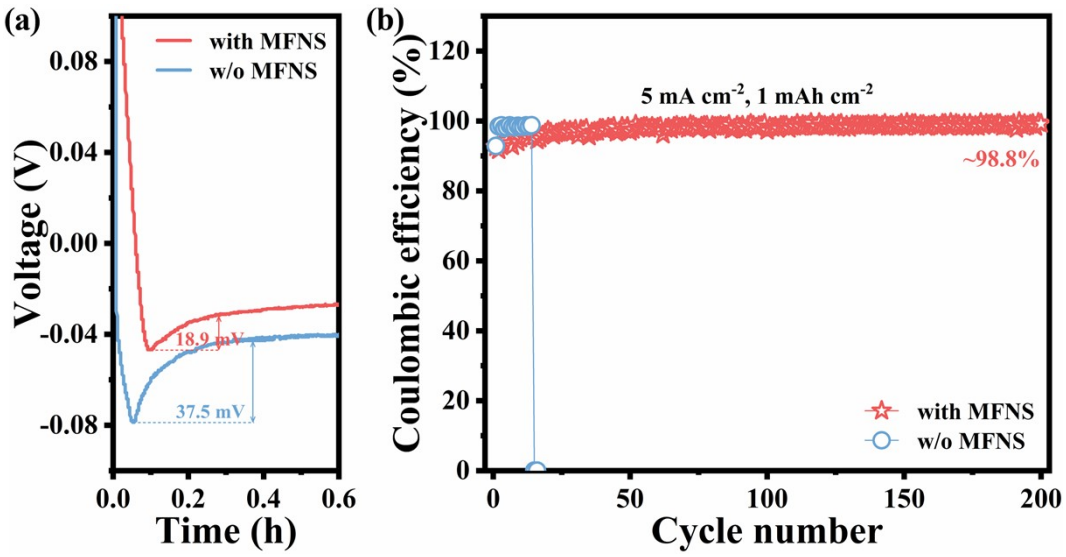

Fig. S3 Electrochemical performance of the Li||Cu asymmetrical half-cells with or without MFNS interlayers. (a) Nucleation overpotential at 1 mA cm^{-2}. (b) Coulombic efficiency at 5 mA cm^{-2}/1 mAh cm^{-2}.

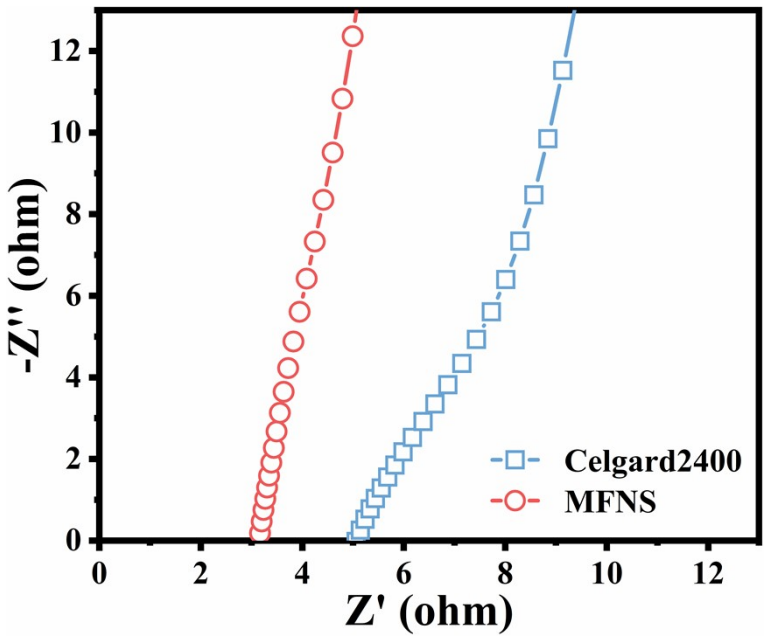

Fig. S4 Nyquist plots of SS||SS symmetric cells with Celgard2400 separator and MFNS.

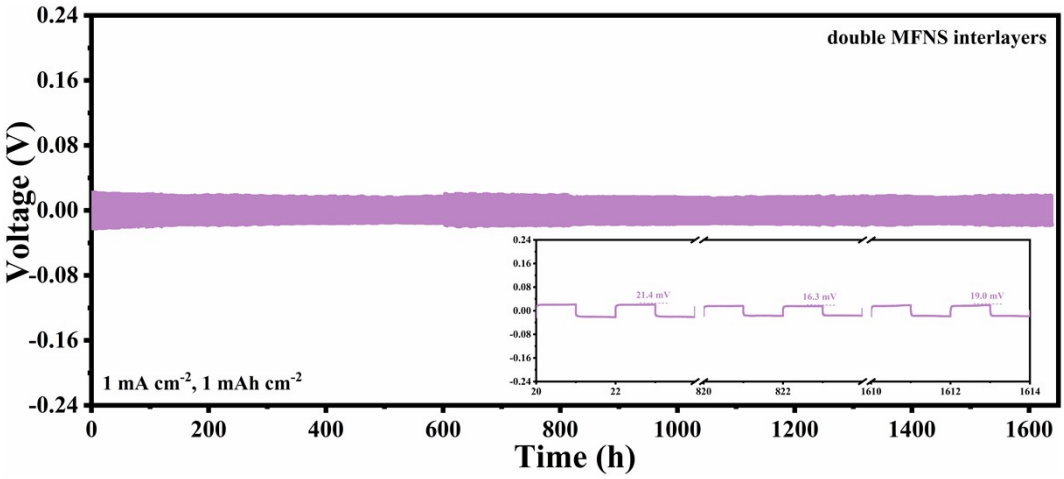

Fig. S5 Galvanostatic discharge-charge voltage profiles of the Li||Li symmetric cell with double MFNS interlayers at 1 mA cm^{-2}/1 mAh cm^{-2}.

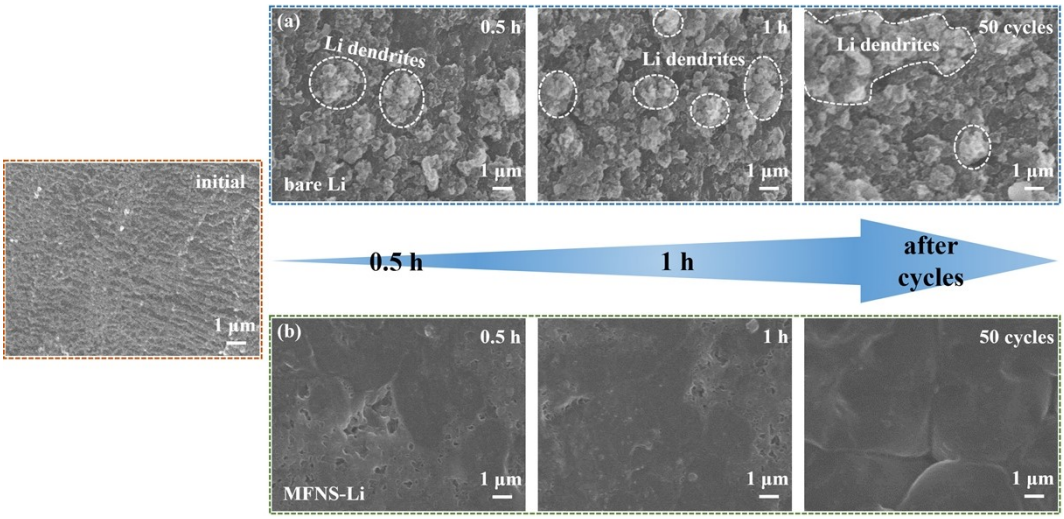

Fig. S6 SEM images of morphological evolution for (a) bare Li and (b) MFNS-Li after Li deposition at 1 mA cm^{-2}.

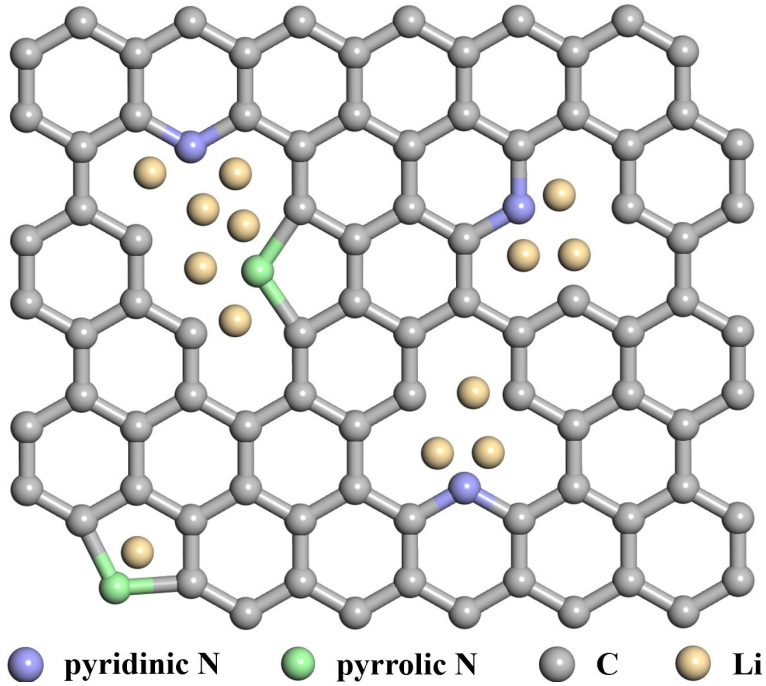

Fig. S7 Attraction of Li^+ by pyridinic N and pyrrolic N enriched in MFNS.

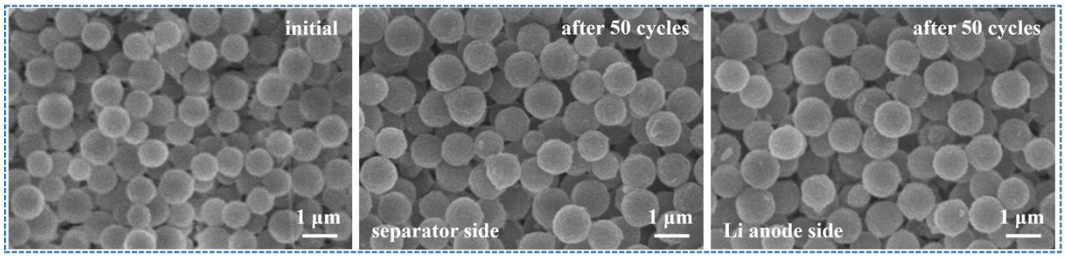

Fig. S8 SEM images of morphological evolution for MFNS interlayer after Li deposition at 1 mA cm^{-2}/ 1 mAh cm^{-2}.

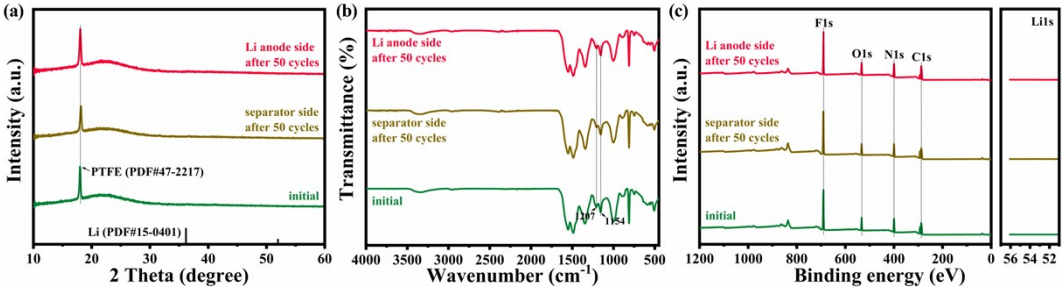

Fig. S9 Structure characterization of MFNS interlayers at various status. (a) XRD patterns, (b) FTIR spectrums, and (c) overall XPS spectrums.

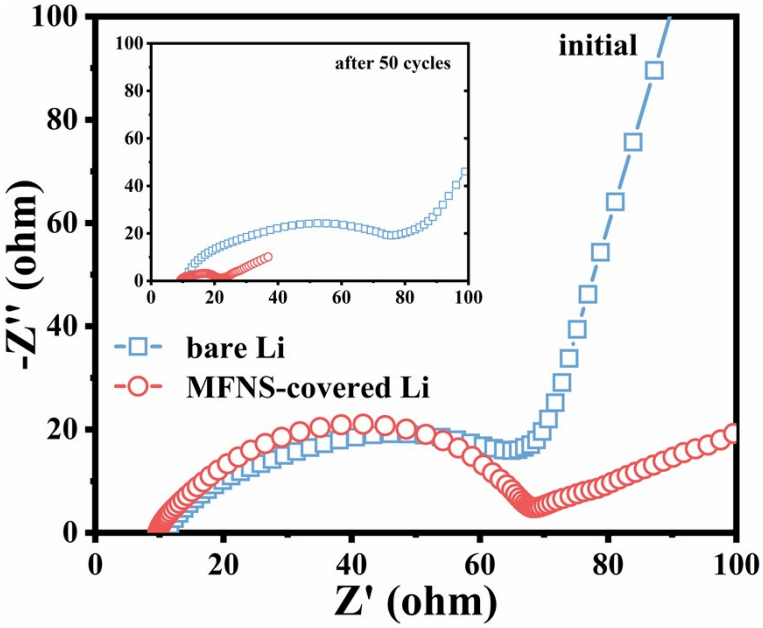

Fig. S10 Nyquist plots of Li||LFP cells before and after 50 cycles (inset) at 1 C.

As shown in Fig. S10, in the initial state, the interfacial resistance of the MFNS-covered Li||LFP cell is close to that of the bare Li||LFP cell, which indicates that the introduction of the interlayer does not prolong the Li^+ transport path. However, the interfacial resistance of the bare Li||LFP cell increased significantly after 50 cycles, which was mainly due to the severe surface corrosion of the bare Li electrode and the increase of side reactions during the cycling process, resulting in "dead Li". On the contrary, the MFNS interlayer inhibited the side reactions on the Li metal surface and greatly extended the cycle life of the cell.

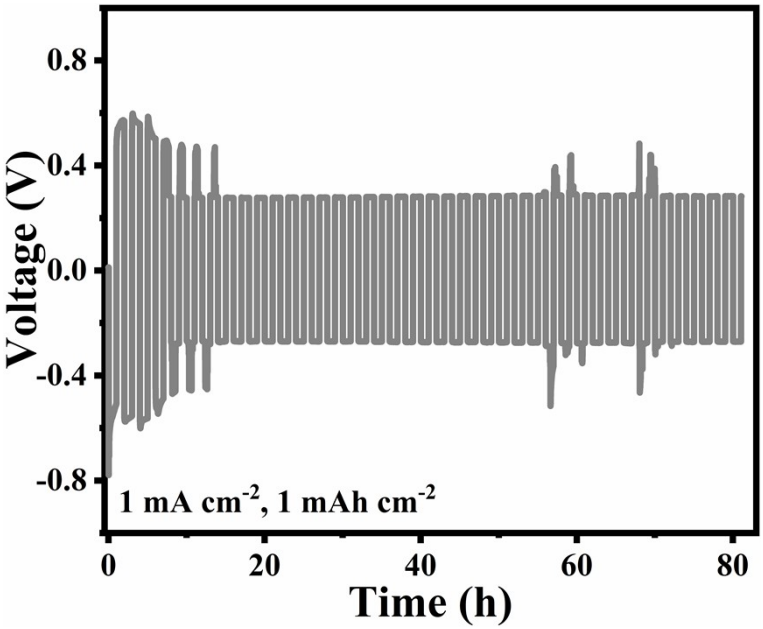

Fig. S11 Galvanostatic discharge-charge voltage profiles of the Li||Li symmetric cell with MFNS separator at 1 mA cm^{-2}/1 mAh cm^{-2}.

In order to verify the possibility of MFNS to replace conventional PP separator, Li||Li symmetric cell with MFNS separator was assembled and tested. Unfortunately, as shown in Fig. S11, the polarization voltage was as high as 300 mV with great fluctuations under the condition of 1 mA cm^{-2}/1 mAh cm^{-2}.

Table S1. Atomic percentage of C, N, and O elements for MFNS.

Materials	C (%)	N (%)	O (%)
MCCI	60.7	22.2	17.1

Table S2. Atomic percentage of C, N, O, F, and Li elements for MFNS interlayers at various status.

Status	C (%)	N (%)	O (%)	F (%)	Li (%)
initial	44.7	18.7	9.5	27.1	-
separator side after 50 cycles	44.1	17.2	8.5	30.2	-
Li anode side after 50 cycles	45.8	17.8	10	26.4	-

Table S3. Polarization voltage of full cells with or without MFNS interlayer at different current densities.

	0.1 C	0.2 C	0.3 C	0.5 C	1.0 C	2.0 C	3.0 C
with MFNS	54.8 mV	62.8 mV	73.5 mV	104.5 mV	149.1 mV	238.1 mV	328.3 mV
w/o MFNS	113.8 mV	131.5 mV	134.2 mV	164.0 mV	238.1 mV	486.8 mV	564.2 mV